

# Efficiency of the Multicanonical Simulation Method as Applied to Peptides of Increasing Size: The Heptapeptide Deltorphin

FATİH YAŞAR,<sup>1</sup> HANDAN ARKIN,<sup>1</sup> TARIK ÇELİK,<sup>1</sup> BERND A. BERG,<sup>2</sup> HAGAI MEIROVITCH<sup>3</sup>

<sup>1</sup>Department of Physics Engineering, Hacettepe University, 06532, Ankara, Turkey

<sup>2</sup>Department of Physics, Florida State University, Tallahassee, Florida 32306

<sup>3</sup>School of Computational Science and Information Technology, Florida State University, Tallahassee, Florida 32306, and Center for Computational Biology and Bioinformatics, School of Medicine, University of Pittsburgh, Pennsylvania 15213

Received 20 November 2001; Accepted 1 April 2002

**Abstract:** The advantage of the multicanonical (MUCA) simulation method of Berg and coworkers over the conventional Metropolis method is in its ability to move a system effectively across energy barriers thereby providing results for a wide range of temperatures. However, a MUCA simulation is based on weights (related to the density of states) that should be determined prior to a production run and their calculation is not straightforward. To overcome this difficulty a procedure has been developed by Berg that calculates the MUCA weights automatically. In a previous article (Yaşar et al. *J Comput Chem* 2000, 14, 1251–1261) we extended this procedure to continuous systems and applied it successfully to the small pentapeptide Leu-enkephalin. To investigate the performance of the automated MUCA procedure for larger peptides, we apply it here to deltorphin, a linear heptapeptide with bulky side chains (H-Tyr<sup>1</sup>-D-Met<sup>2</sup>-Phe<sup>3</sup>-His<sup>4</sup>-Leu<sup>5</sup>-Met<sup>6</sup>-Asp<sup>7</sup>-NH<sub>2</sub>). As for Leu-enkephalin, deltorphin is modeled in vacuum by the potential energy function ECEPP. MUCA is found to perform well. A weak second peak is seen for the specific heat, which is given a special attention. By minimizing the energy of structures along the trajectory it is found that MUCA provides a good conformational coverage of the low energy region of the molecule. These latter results are compared with conformational coverage obtained by the Monte Carlo minimization method of Li and Scheraga.

© 2002 Wiley Periodicals, Inc. *J Comput Chem* 23: 1127–1134, 2002

**Key words:** deltorphin; Metropolis Monte Carlo; multicanonical simulation; proteins; peptides; thermodynamic averages; energy minimization

## Introduction

Biological macromolecules such as proteins have a well-defined 3D structure that is essential for their biological activity. Therefore, predicting the protein's structure by theoretical/computational methods is an important goal in structural biology.<sup>1</sup> The atomic interactions of a protein are commonly modeled by an empirical potential energy function (force field), which typically leads to a complex energy profile consisting of a tremendous number of local minima; their basins of attraction have been called *localized microstates*. The energy profile also contains larger potential energy wells defined over *wide microstates* (e.g., the protein's fluctuations around its averaged structure), each including many localized ones.<sup>2</sup> Molecular dynamics (MD)<sup>3</sup> simulations have shown that a system will stay in a localized microstate for a very short time (several femtoseconds) while spending much longer times in a wide microstate;<sup>4</sup> therefore, the latter are of the

greater experimental interest. For a perfect force field (which also takes into account the effect of the solvent) the most stable wide microstate corresponds to the native structure. However, because of energy barriers, the commonly used thermodynamic simulation techniques such as the Metropolis Monte Carlo (MC)<sup>5</sup> and molecular dynamics are very inefficient at 300 K; thus, the molecule remains in its starting wide microstate or moves to a neighboring wide microstate, but in practice, will never reach the most stable

**Correspondence to:** H. Meirovitch; e-mail: hagaim@pitt.edu

Contract/grant sponsor: Doe; contract/grant numbers: DE-FG05-95ER62070 (H.M.) and DE-F602-97ER41022 (B.B.)

Contract/grant sponsor: NIH; contract/grant number: R01GM61916-02 (H.M.)

Contract/grant sponsor: Hacettepe University Research Fund; contract/grant number: 00.01.602.001

one. Therefore, developing *statistical mechanics* simulation methods that lead to an efficient crossing of the energy barriers has been a long-standing challenge.

Peptides, which are much more flexible than proteins, are typically random coils, but for certain solvents and temperature conditions might undergo intermediate flexibility, where several wide microstates are populated significantly in thermodynamic equilibrium. One then seeks to identify the most stable wide microstates and to calculate their populations. For peptides, the MC or MD methods suffer from the same limitation mentioned above with regard to proteins, and a common alternative has been a two-stage approach in which the wide microstates are identified initially by an extensive conformational search for low-energy minimized structures, and each microstate is then spanned by an MC or an MD simulation. The free energy of these microstates, which leads to the populations, can be calculated by the harmonic approximation<sup>6–8</sup> or by the local states method,<sup>9</sup> for example. Therefore, development of efficient methods for conformational search is desirable as well.<sup>10,11</sup> Most of the methodologies for treating intermediate flexibility have been developed for the analysis of nuclear magnetic resonance (NMR) structural data of flexible peptides (see, e.g., refs. 2 and 12, and references cited in ref. 11).

The trapping problem of the MC and MD methods can be alleviated to a large extent by the multicanonical (MUCA) MC method of Berg and collaborators,<sup>13–15</sup> which was applied initially to lattice spin models, and its relevance for complex systems was first noticed in ref. 14. Application of MUCA to peptides was pioneered by Hansmann and Okamoto<sup>16</sup> and followed by others;<sup>17</sup> simulations of protein folding with MUCA and related generalized ensemble methods are reviewed in refs. 18 and 19.

The MUCA ensemble (unlike a Boltzmann ensemble) is based on a probability function in which the different energies are equally probable. For a discrete system, the probability of configuration  $\mathbf{x}$  of energy  $E$  is

$$P^{\text{MU}}(\mathbf{x}) = \frac{1}{Ln(E_{\mathbf{x}})} = \frac{\exp[-S(E_{\mathbf{x}})/k_B]}{L} \quad (1)$$

where  $L$  is the number of different energy levels of the system,  $n(E_{\mathbf{x}})$  is the multiplicity of energy  $E_{\mathbf{x}}$  and  $S(E_{\mathbf{x}}) = k_B \ln n(E_{\mathbf{x}})$  is the entropy of the microcanonical ensemble at energy  $E_{\mathbf{x}}$  (microcanonical entropy). In practice  $L$  will be defined also for a continuum system because a finite energy range will be divided into  $L$  small segments. The MC process based on this probability distribution is

$$p_{x,y} = \min[1, n(E_{\mathbf{x}})/n(E_{\mathbf{y}})] = \min[1, \exp(S(E_{\mathbf{x}})/k_B - S(E_{\mathbf{y}})/k_B)] \quad (2)$$

where  $p_{x,y}$  is the transition probability to select configuration  $\mathbf{y}$  with energy  $E_{\mathbf{y}}$  following the preceding selection of configuration  $\mathbf{x}$  with energy  $E_{\mathbf{x}}$ . The system visits the different energies approximately for equal amounts of times and the trapping problem mentioned above is improved. However, implementation of MUCA is not straightforward because the density of states  $n(E)$  is

unknown *a priori*. In practice, one only needs to know the weights  $\omega$ ,

$$w = w(E) \sim 1/n(E) = \exp[-S(E)/k_B] = \exp[(E - F_{T(E)})/k_B T(E)] \quad (3)$$

because only ratios of  $n(E)$  appear in eq. (2). These weights are calculated in the first stage of a MUCA process by an iterative procedure in which the temperatures  $T(E)$  are built recursively together with the microcanonical free energies  $F_{T(E)}/k_B T(E)$ , up to an additive constant. The iterative procedure is followed by a long production run based on the fixed  $w$ s, where equilibrium configurations are sampled. Reweighting techniques (see Ferrenberg and Swendsen<sup>20</sup> and literature given in their second reference) enable one to obtain Boltzmann averages of various thermodynamic properties over a large range of temperatures.

As pointed out above, calculation of the *a priori* unknown MUCA weights is not trivial, requiring an experienced human intervention that has been a stumbling block for newcomers to the method. An alternative way is to establish an automatic process by incorporating all the assembled statistical within the recursion procedure. For lattice models, this problem was addressed in a sketchy way by Berg and Celik<sup>14</sup> and later by Berg,<sup>21,22</sup> but no extension to continuum peptide models has been carried out with the exception of a recent article<sup>23</sup> where it is simply stated that the recursion of ref. 22 has been used. In a more recent article we have provided a detailed translation of this recursion procedure for simulations of continuum models of peptides and proteins.<sup>24</sup> The procedure was tested successfully as applied to models of the pentapeptide Leu-enkephalin (H-Tyr-Gly-Gly-Phe-Leu-OH) described by the ECEPP/2 potential energy function.<sup>25</sup>

To verify the coverage of the low-energy region by the MUCA sample, we also minimized the energy of selected conformations of the trajectory and indeed recovered the global energy minimized structure and other low-energy minimized structures.<sup>24</sup> This suggests that MUCA can also serve as a useful conformational search technique for identifying the most stable wide microstates of a peptide, as discussed earlier. Although these MUCA results are very satisfactory, it should be pointed out that they are based on a selection of candidate structures for energy minimization, which is based on the canonical ensemble of statistical physics. More conformational structures were found with the Monte Carlo minimization (MCM) method of Li and Scheraga.<sup>26</sup>

In view of these encouraging MUCA results, it would be of interest to study its efficiency as applied to molecules of increasing size, and in particular, to examine the performance of its automatic recursion procedure (many of the previous studies of MUCA were applied to relatively small peptides such as the pentapeptides Met-enkephalin<sup>16,27–29</sup> and Leu-enkephalin;<sup>24</sup> a larger molecule studied is poly-alanine, a homopolymer with small side chains,<sup>30,31</sup> and the 13-residue C-peptide of Ribonuclease A.<sup>32</sup> A first step in this direction is carried out in this article where MUCA is applied to a linear heptapeptide with bulky side chains, deltorphin (also known as dermenkephalin) (H-Tyr<sup>1</sup>-D-Met<sup>2</sup>-Phe<sup>3</sup>-His<sup>4</sup>-Leu<sup>5</sup>-Met<sup>6</sup>-Asp<sup>7</sup>-NH<sub>2</sub>). This natural peptide found in frog skin, has high potency and receptor selectivity for  $\delta$  opioid receptors. To understand the conformation–activity relationships, NMR studies

of the solution structures of deltorphin in DMSO and cryoprotective solvents were carried out<sup>33</sup> and computational work was based on these experiments.<sup>34</sup>

In this work, as in our previous one,<sup>24</sup> deltorphin is modeled by the ECEPP/2 potential, which assumes a rigid geometry (i.e., constant bond lengths and angles), and is based on Lennard–Jones, torsional, hydrogen bond, and electrostatic potentials, where the dielectric constant is  $\epsilon = 2$  (see ref. 25). Thus, a conformation is defined solely by the dihedral angles, whose number increases from 19 (for constant  $\omega = 180^\circ$ ) and 24 (variable  $\omega$ ) for Leu-enkephalin, to 36 (constant  $\omega$ ) for deltorphin; the latter consist of the 14 backbone  $\phi$  and  $\psi$  and the 22 side chain angles  $\chi$ . ECEPP is implemented in the package FANTOM,<sup>35</sup> which is used in the present simulations. Because ECEPP does not consider solvent effects, we do not attempt to compare our results to experimental NMR data and only study the efficiency of MUCA as a thermodynamic simulation technique as well as a conformational search tool for locating low energy minimized structures compared with MCM.<sup>26</sup>

Also, as in our previous work,<sup>24</sup> at each MC step a single dihedral angle is treated where its trial value is obtained at random within the range  $[-180^\circ, 180^\circ]$ ; the 36 dihedral angles of the molecule are visited in a predefined order, going from Tyr to Asp, where such a cycle of  $n$  MC steps ( $n = 36$ ) defines a sweep. In ref. 24 we have found that the efficiency of MUCA is decreased if the above range is decreased to  $[-90^\circ, 90^\circ]$ ; changing several angles at each MC step has led to a considerable decrease in the performance as well. However, as the molecular size increases, the choice of the trial conformations is expected to affect the ability of the process to reach the low-energy region in conformation space. This has already been noticed by Hao and Scheraga,<sup>17b</sup> who have selected trial conformations with a bias for generating low-energy conformations.

Details about the implementation of MUCA are given in ref. 24. Here, we only provide a very brief description of the process. The MUCA weights are a step function of the energy<sup>13</sup>

$$w_i(\mathbf{x}) = \exp(-b_i E_x + a_i) \quad \text{for } E_{i-1} < E_x \leq E_i \quad (4)$$

where the  $b_i$  are inverse microcanonical temperatures,  $b_i = (k_B T_i)^{-1}$ , and the  $a_i$  are related to microcanonical free energies. The  $a_i$  are not independent, but follow from the  $b_i$ . For the determination of the  $b_i$  we use the recursion<sup>21</sup> in its extension to continuum peptides.<sup>24</sup> It relies on  $m = 1, 2, \dots$  short runs with weights determined by  $b_i^{m-1}$  and the iteration from  $m - 1$  to  $m$  is

$$b_{i-1}^m = b_{i-1}^{m-1} + \hat{g}_{i-1}^m \ln[H_{i-1}^m/H_i^m]/\Delta E_i. \quad (5)$$

Here, the  $H_i^m$  are (not yet used) energy histograms for the range  $E_{i-1} \leq E \leq E_i$ , and the statistical factor  $\hat{g}_{i-1}^m$  incorporates information about all runs up to  $m$ . In particular,  $\hat{g}_{i-1}^m$  is zero if either  $H_{i-1}^m$  or  $H_i^m$  is zero, such that the proper limit of  $\hat{g}_{i-1}^m \ln[H_{i-1}^m/H_i^m]$  is also zero in that situation.

## Results and Discussion

We first carried out canonical (i.e., constant  $T$ ) MC simulations at relatively high temperatures and MUCA test runs, which enabled

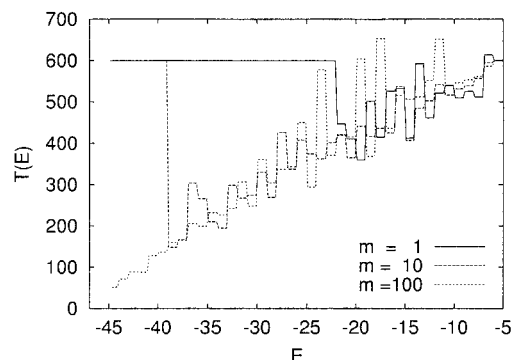


**Figure 1.** Development of the temperature functions  $T^n(E)$  under the multicanonical recursion.

us to determine the required energy ranges. Then we performed full MUCA simulations, which cover reliably the high-temperature region up to  $T_{\max} = 600$  K. In these simulations the energy range,  $[-4, -44]$  kcal/mol was divided into 40 bins of 1 kcal/mol each, where for energies above  $-4$  kcal/mol the same temperature,  $T_{\max} = 600$  K was used; the lowest energy encountered was  $-43.35$  kcal/mol.

The MUCA weights were built recursively during a long *single* simulation of  $10^6$  sweeps, where the parameters  $b_i$  and  $a_i$  were iterated every 5000 sweeps. Figure 1 depicts how the recursion works. The simulation is started in the disordered region with an initial temperature (step) function of  $T_i = 600$  K for all the segments  $[E_{i-1}, E_i]$  and the figure shows the decrease of the temperature factors  $T_i = (b_i k_B)^{-1}$  after  $m = 1, 10$ , and 100 recursions. The  $T_i$  values penetrate deeper and deeper into the ordered, low-energy region as  $m$  increases. For low, but not yet reached energies,  $T_i$  remains on the 600 K line. After 100 recursions this no longer happens, because the lowest energy bin, which contains the ground state has been reached.

Having fixed the MUCA weight factors, a MUCA production run was carried out with  $10^6$  sweeps (the first 200,000 sweeps were used for thermalization). Figure 2 shows a typical time series, more precisely, 1/5 of the entire trajectory of the simulation. From the MUCA production run canonical ensemble expectation values of thermodynamic quantities were obtained by reweighting,<sup>20</sup>

$$\bar{E}(T) = \frac{\sum_i E_i \exp(-\beta E_i + b_i E_i - a_i)}{\sum_i \exp(-\beta E_i + b_i E_i - a_i)} \quad (6)$$

where each subscript is  $i = i(t)$  such that  $E_{i-1} \leq E_t < E_i$ . Figure 3 shows the canonically reweighted energy  $E$  as a function of  $T$ . Compared with the multicanonical results are the expectation values of the energy from canonical simulations of  $10^5$  sweeps each, at temperatures within the range 50 to 400 K. It is clear that at high temperature the agreement is excellent, whereas the canonical simulations fail to equilibrate at the low temperature region.

In Figure 4 we show our data for the specific heat  $C$ , which is calculated from the energy fluctuations,

$$C(T) = \frac{1}{7k_B T} (\langle E^2 \rangle_T - \langle E \rangle_T^2) \quad (7)$$

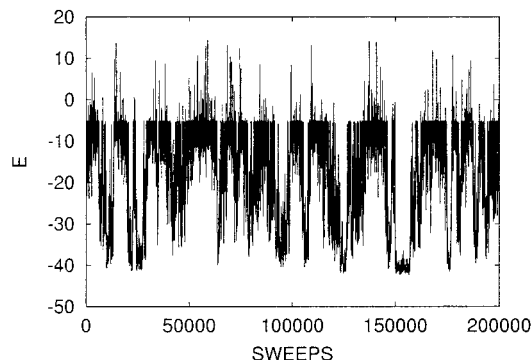


**Figure 2.** Time series of the multicanonical simulation.

where 7 is the number of amino acids. The peak of  $C$  appears at  $T_{\max} \sim 450$  K, which is a significantly higher temperature than the corresponding value,  $\sim 300$  K obtained for the specific heat peak of Met-enkephalin<sup>16</sup> and Leu-enkephalin.<sup>24</sup> This is an expected behavior because as the molecule's size,  $N$ , increases the ground state (or the several ground states) becomes stabilized by a larger number ( $\sim N^2$ ) of long-range interactions and a higher temperature is required to move the molecule from the ordered to the disordered region; a similar behavior has been observed for lattice models of trails<sup>36,37</sup> as well as continuum models of poly-alanine.<sup>30,31</sup>

The second interesting feature of Figure 4 is the existence of a much smaller second peak in the neighborhood of  $T \sim 200$  K. It should be pointed out that initially this peak was significantly larger based on energy fluctuations obtained from a single MUCA run of  $10^6$  sweeps. To check whether this peak has physical meaning or it is a result of insufficient sampling, we carried out three additional MUCA simulations of equal length, and the specific heat curve in Figure 4 is based on a larger sample of  $4 \times 10^6$  sweeps. The fact that the height of the second peak in Figure 4 has been reduced significantly suggests that the occurrence of the original peak probably stems from poor statistics. This conclusion is important because two and three peaks in the specific heat have also been obtained in other simulations of chain models. A recent study of the C-peptide of ribonuclease A suggests that for a

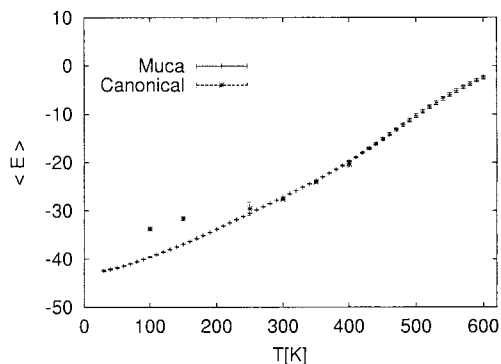


**Figure 3.** The Boltzmann average energy as a function of temperature: multicanonical vs. canonical simulations.

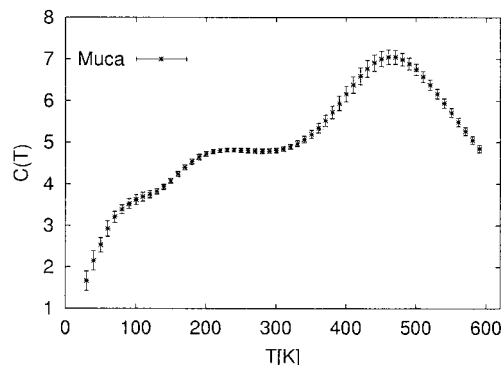


**Figure 4.** Specific heat from multicanonical simulations as a function of the temperature.

heteropolymers two separate transition temperatures may exist.<sup>32</sup> Studying an isotropic homopolymers, Zhou et al.<sup>38</sup> have observed a second peak in the heat capacity that they have identified as a solid-solid transition accompanying the crystallization into the ground state. The occurrence of multiple phase transitions is also reported for worm-like polymer chains.<sup>39</sup>

In summary, the use of the multicanonical histogram recursion has proven to be a convenient way for an automatic generation of the MUCA weights for the five residue Leu-enkephalin studied previously as well as for the present seven-residue deltorphin. Notice, however, that the number of sweeps required for the automatic procedure appears to be larger than that commonly used in a manual building of the weights, i.e., by human intervention after each iteration. Also, to obtain statistically reliable samples for the specific heat, the required sample size has been increased from  $6 \times 10^5$  for Leu-enkephalin to  $4 \times 10^6$  for deltorphin.

### Energy Minimization

As pointed out in the Introduction, for peptides it is not only of interest to obtain thermodynamic averages and fluctuations at different temperatures but also to find the most stable regions in the conformational space, which allows one to identify the most stable wide microstates. In the organic chemistry community conformational search methods have been developed, and attempts have been made to find the global energy minimum and all the energy minimized structures in certain energy ranges above the GEM [see refs. 10 and 2(b), and references cited therein]. Therefore, as in ref. 24, it is of interest to investigate the conformational coverage provided by MUCA, in particular in the low-energy region.

We energy minimized (quenched) the configurations generated in  $10^5$  sweeps of the MUCA production run. The minimized structures were sorted according to a variance criterion where two structures are considered to be different if at least one dihedral angle differs by more than  $2^\circ$ . The lowest energy found (our suspected GEM) is

$$E = -44.1058 \text{ kcal/mol} \quad (8)$$



**Figure 5.** The conjectured GEM structure with energy defined in eq. (8). The figure was created by VMD.

and its conformation is depicted in Figure 5, where the last four residues are shown to pertain to the  $\alpha$ -helical region. The number of structures found in energy bins of 0.5 kcal/mol above  $E = -44.11$  kcal/mol appear in Table 1. As in ref. 24, we compare the conformational coverage of the low-energy region to that obtained with MCM.<sup>26</sup> Because the efficiency of MCM strongly depends on the temperature,<sup>41</sup> we carried out three different MCM simulations each of  $10^5$  steps at  $T = 300, 400,$  and  $600$  K, where only the results for the last two temperatures are presented in Table 1. Indeed, the two MCM runs have led to significantly different results, where the highest population of the five lowest energy bins is obtained with MCM (400 K), while (as expected) in most cases MCM (600 K) leads to the largest population of the higher energy bins (6–13). The populations of bins 1–4 obtained with MCM (300 K) are between those of MCM (600 K) and MCM (400 K). Although the populations of MUCA are always smaller than the corresponding populations obtained with MCM (400 K), for bin 1

the results of the two methods are very close, which means that a very good coverage of the lowest energy bin is provided by MUCA. This is important, due to the fact that MUCA covers a large range of energies in an approximately homogeneous way, while with MCM (400 K) a strong preference is given for simulating the low energy region. Therefore, it is expected that minimizing the energy of a larger number of MUCA structures (which for peptides is not a very time consuming calculation) would lead to a significant increase in the MUCA populations of all the bins.

MUCA is most important as being a thermodynamic method that enables simulating a system over a large range of temperatures. This aspect is demonstrated in Figure 6, where Ramachandran plots of typical structures for three temperature ranges are presented. The first set of seven plots (for the seven amino acid residues) is for the GEM structure and structure pertaining to the lowest energy bin above the GEM (bin 1 in Table 1). The second and third sets show the most probable structures for two temperature regions, 130–140 K and 290–300 K, respectively. The figure reveals that already the second set contains structures that do not belong to the wide microstate of the GEM structure (i.e., some of their  $\phi$  and  $\psi$  deviate by more than  $60^\circ$  from the values of the GEM structure); this is mainly pronounced for the end residues Tyr and Asp that are expected to be the most flexible. However, for each residue *most* of the structures still belong to the wide microstate of the GEM structure, as expected for a low enough temperature.

The scattering of points increases significantly for  $T = 290$ – $300$  K, suggesting that deltorphin modeled with the ECEPP potential will populate at least several wide microstates at room temperature. In particular, the last four residues, which for the GEM structure reside in the  $\alpha$ -helix region become mostly populated in the extended region. The fact that such a scatter of structures occurs at a temperature significantly below the transition temperature,  $T_C \sim 450$  K, reflects the wide peak of the specific heat (see Fig. 4), which stems from the small size of the present peptide; only for a large protein a collapse is expected to occur

**Table 1.** Number of Energy-Minimized Structures in Energy Bins of 0.5 kcal/mol above  $E = -44.11$  kcal/mol as Obtained by the MUCA and the MCM Methods.

Bin (kcal/mol)	Energy (kcal/mol)	Muca	MCM	
			$T = 600$ K	$T = 400$ K
0.0–0.5	–44.11 to –43.61	683	252	769
0.5–1.0	–43.61 to –43.11	883	936	2165
1.0–1.5	–43.11 to –42.61	1532	1889	3367
1.5–2.0	–42.61 to –42.11	906	3229	4754
2.0–2.5	–42.11 to –41.61	1253	4077	4685
2.5–3.0	–41.61 to –41.11	1417	4765	4581
3.0–3.5	–41.11 to –39.61	1807	5396	3931
3.5–4.0	–39.61 to –39.11	1381	6083	3329
4.0–4.5	–39.11 to –38.61	1515	5861	3394
4.5–5.0	–38.61 to –38.11	1340	6109	5044
5.0–5.5	–38.11 to –37.61	1227	5560	6513
5.5–6.0	–37.61 to –37.11	1227	5302	4417
6.0–6.5	–37.11 to –36.61	1332	5157	4037

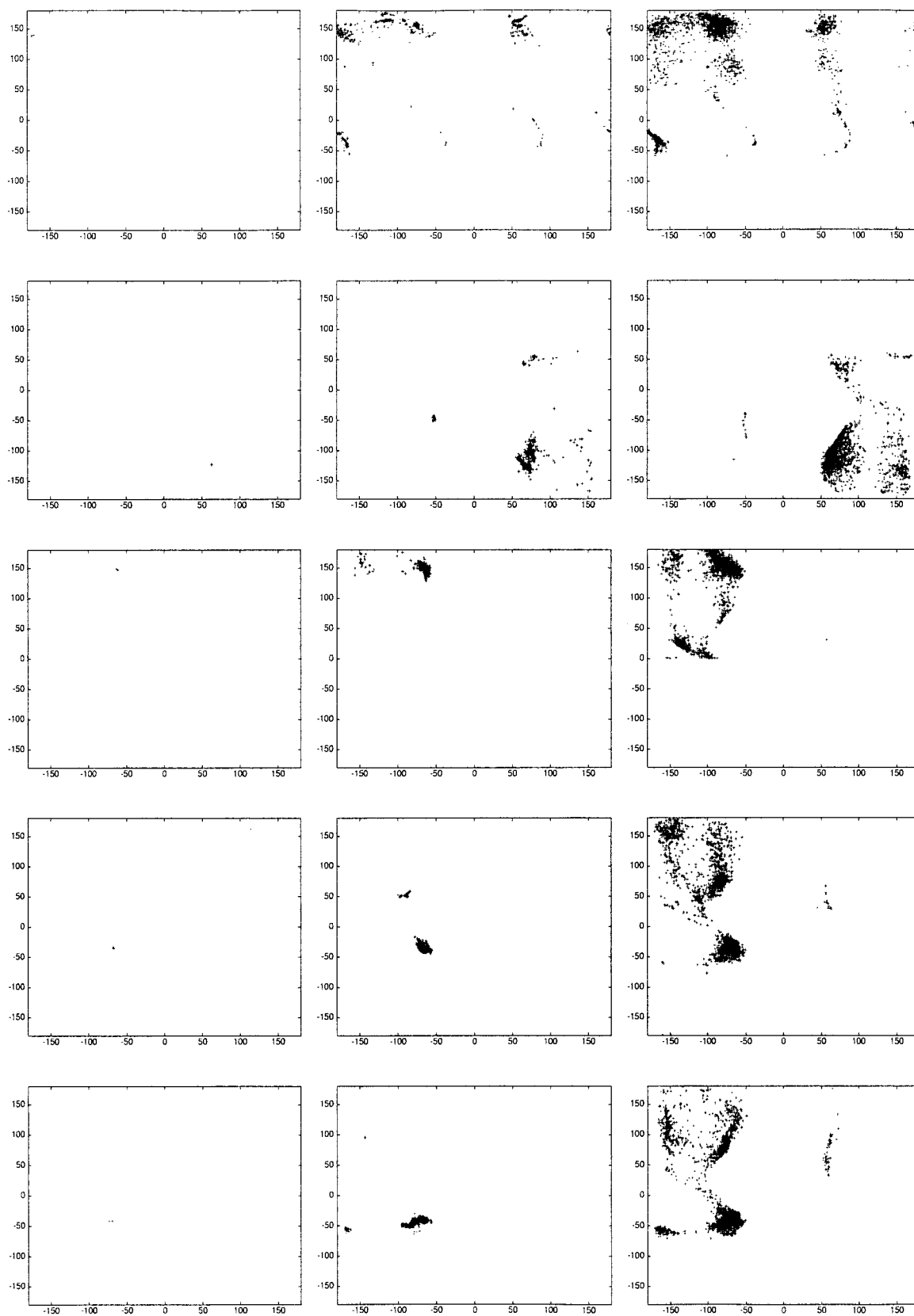


**Figure 6.** Ramachandran plots of each residue (from top to bottom) Tyr<sup>1</sup>-D-Met<sup>2</sup>-Phe<sup>3</sup>-His<sup>4</sup>-Leu<sup>5</sup>-Met<sup>6</sup>-Asp<sup>7</sup>. The abscissa is the angle  $\phi$  and the ordinate is  $\psi$ . The first column shows the GEM structure and the conformations of the lowest energy bin of Table 1; the middle column shows typical conformations for the temperature range 130–140 K, and the last column typical conformations for the range 290–300 K.

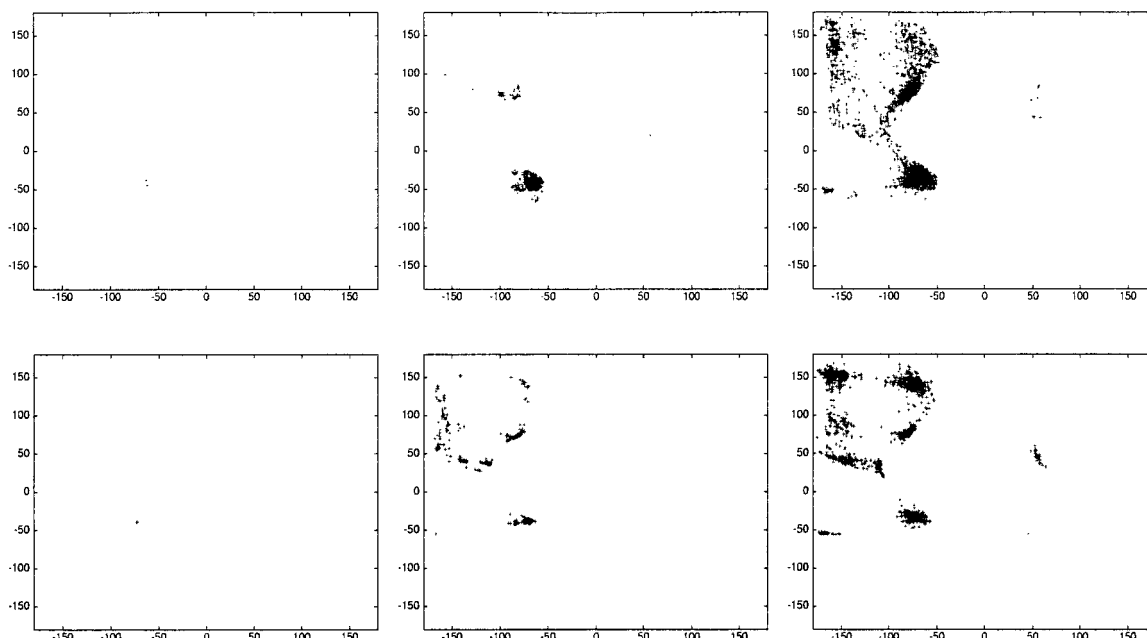


Figure 6. (Continued)

below and relatively close to  $T_C$ . Indeed, a small linear peptide at room temperature in general does not populate a single wide microstate, and analysis of NMR data of deltorphin in DMSO suggests that several wide microstates are populated significantly in thermodynamic equilibrium.<sup>34</sup> Because the ECEPP potential used here is not expected to model correctly a peptide in DMSO we have not attempted to compare our results at 300 K to the NMR data.

In summary, the objective of this work has been to investigate the performance of the MUCA method based on the automatic recursive procedure for peptides introduced by us in ref. 24. There, MUCA was applied preliminarily to the small pentapeptide Leu-enkephalin, while here we simulate the larger peptide, deltorphin, which consists of seven residues with bulky side chains. We find the multicanonical method to work in precisely the same way as for Leu-enkephalin; however, the computer time needed increased by about one order of magnitude. Thus, the 12 h required for a production run of Leu-enkephalin, become about 1 week for deltorphin (using a DEC-Alpha 433 MHz workstation). By brute force and involving parallelization techniques an extension of such simulations by three orders of magnitude, seems to be in reach, which will allow treating much larger systems. Also, to enhance the efficiency of MUCA for larger peptides it might be necessary to apply a biased selection of conformations, which can be carried out, for example, with the scanning construction procedure.<sup>42</sup>

### Acknowledgments

The simulations were performed on alpha workstations of the Hacettepe University.

### References

- Vásquez, M.; Némethy, G.; Scheraga, H. A. *Chem Rev* 1994, 94, 2183.
- (a) Meirovitch, H.; Meirovitch, E. *J Phys Chem* 1996, 100, 5123; (b) Baysal, C.; Meirovitch, H. *Biopolymers* 1999, 50, 329.
- (a) Alder, B. J.; Wainwright, T. E. *J Chem Phys* 1957, 27, 1209; (b) McCammon, J. A.; Gelin, B. R.; Karplus, M. *Nature* 1977, 267, 585.
- (a) Stillinger, F. H.; Weber, T. A. *Science* 1984, 225, 983; (b) Elber, R.; Karplus, M. *Science* 1987, 235, 318.
- Metropolis, N.; Rosenbluth, A. W.; Rosenbluth, M. N.; Teller, A. H.; Teller, E. *J Chem Phys* 1953, 21, 1087.
- (a) Gō, N.; Scheraga, H. A. *J Chem Phys* 1969, 51, 4751; (b) Gibson, K. D.; Scheraga, H. A. *Physiol Chem Phys* 1969, 1, 109; (c) Gō, N.; Scheraga, H. A. *Macromolecules* 1976, 9, 535.
- Hagler, A. T.; Stern, P. S.; Sharon, R.; Becker, J. M.; Naider, F. *J Am Chem Soc* 1979, 101, 6842.
- (a) Karplus, M.; Kushick, J. N. *Macromolecules* 1981, 14, 325; (b) Case, D. A. *Curr Opin Struct Biol* 1994, 4, 285.
- (a) Meirovitch, H. *Chem Phys Lett* 1977, 21, 389; (b) Meirovitch, H.; Vásquez, M.; Scheraga, H. A. *Biopolymers* 1987, 26, 651; (c) Meirovitch, H.; Koerber, S. C.; Rivier, J.; Hagler, A. T. *Biopolymers* 1994, 34, 815.
- (a) Saunders, M. *J Am Chem Soc* 1987, 109, 3150; (b) Saunders, M. *J Comput Chem* 1991, 12, 645; (c) Gotō, H.; Ōsawa, E. *J Am Chem Soc* 1989, 111, 8950; (d) Gotō, H.; Ōsawa, E. *Tetrahedron Lett* 1992, 33, 1343; (e) Chang, G.; Guida, W. C.; Still, W. C. *J Am Chem Soc* 1989, 111, 4379; (f) Saunders, M.; Houk, K. N.; Wu, Y.-D.; Still, W. C.; Lipton, M.; Chang, G.; Guida, W. C. *J Am Chem Soc* 1990, 112, 1419; (g) Braun, W. *Biopolymers* 1987, 26, 1691; (h) Goodman, J. M.; Still, W. C. *J Comput Chem* 1991, 12, 1110; (i) Kollosváry, I.; Guida, W. C. *J Am Chem Soc* 1996, 118, 5011.
- Baysal, C.; Meirovitch, H. *J Am Chem Soc* 1998, 120, 800.
- (a) Betins, J.; Nikiporovich, G. V.; Chipens, G. *J Mol Struct (Theo-*

- chem) 1986, 137, 129; (b) Kessler, H.; Griesinger, C.; Lautz, J.; Muller, A.; van Gunsteren, W. F.; Berendsen, H. J. C. *J Am Chem Soc* 1988, 110, 3393; (c) Brüschweiler, R.; Blackledge, M.; Ernst, R. R. *J Biomol NMR* 1991, 1, 3; (d) Cicero, D. O.; Barbato, G.; Bazzo, R. *J Am Chem Soc* 1995, 117, 1027.
13. Berg, B. A.; Neuhaus, T. *Phys Lett B* 1991, 267, 249.
  14. Berg, B. A.; Çelik, T. *Phys Rev Lett* 1992, 69, 2292.
  15. Berg, B. A. *Fields Inst Commun* 2000, 28, 1; cond-mat/9909236.
  16. Hansmann, U. H.; Okamoto, Y. *J Comput Chem* 1993, 14, 1333.
  17. (a) Hao, M.-H.; Scheraga, H. A. *J Phys Chem* 1994, 98, 4940; (b) *J Phys Chem* 1994, 98, 9882; (c) Kolinski, A.; Galazka, W.; Skolnick, J. *Proteins* 1996, 26, 271; (d) Higo, J.; Nakajima, N.; Shirai, H.; Kidera, A.; Nakamura, H. *J Comput Chem* 1997, 18, 2086.
  18. Hansmann, U. H.; Okamoto, Y. *Annu Rev Comp Phys* 1999, 5, 129.
  19. Mitsutake, A.; Sugita, Y.; Okamoto, Y. *Biopolymers (Peptide Sci)* 2001, 60, 96.
  20. (a) Ferrenberg, A. M.; Swendsen, R. H. *Phys Rev Lett* 1988, 61, 2635; (b) 1989, 63, 1658.
  21. Berg, B. A. *J Stat Phys* 1996, 82, 323.
  22. Berg, B. A. *Nucl Phys B (Proc Suppl)* 1998, 63A–C, 982.
  23. Mitsutake, A.; Okamoto, Y. *Chem Phys Lett* 1999, 309, 95.
  24. Yaşar, F.; Çelik, T.; Berg, B. A.; Meirovitch, H. *J Comput Chem* 2000, 21, 1251–1261.
  25. (a) Momany, F. A.; McGuire, R. F.; Burgess, A. W.; Scheraga, H. A. *J Phys Chem* 1975, 79, 2361; (b) Sippl, M. J.; Némethy, G.; Scheraga, H. A. *J Phys Chem* 1984, 88, 6231.
  26. Li, Z.; Scheraga, H. A. *Proc Natl Acad Sci USA* 1987, 84, 6611.
  27. Eisenmenger, F.; Hansmann, U. H. E. *J Phys Chem B* 1997, 101, 3304.
  28. Hansmann, U. H. E.; Okamoto, Y.; Onuchic, J. N. *Protein Struct Funct Genet* 1999, 34, 472.
  29. Hansmann, U. H. E.; Onuchic, J. N. *J Chem Phys* 2001, 115, 1601.
  30. Hansmann, U. H. E.; Okamoto, Y. *J Chem Phys* 1999, 110, 1267.
  31. Alves, N.; Hansmann, U. H. E. *Phys Rev Lett* 2000, 84, 1836.
  32. Hansmann, U. H. E.; Okamoto, Y. *J Phys Chem B* 1999, 103, 1595.
  33. (a) Temussi, P. A.; Picone, D.; Tancredi, T.; Tomatis, R.; Salvadori, S.; Marastoni, M.; Balboni, G. *FEBS Lett* 1989, 247, 283; (b) Tancredi, T.; Temussi, P. A.; Picone, D.; Amodeo, P.; Tomatis, R.; Salvadori, S.; Marastoni, M.; Santagada, V.; Balboni, G. *Biopolymers* 1991, 31, 751.
  34. (a) Nikiforovich, G. V.; Hruby, V. J. *J Biochim Biophys Res Commun* 1990, 173, 521; (b) Nikiforovich, G. V.; Hruby, V. J.; Prakash, O.; Gehrig, C. A. *Biopolymers* 1991, 31, 941; (c) Nikiforovich, G. V.; Prakash, O.; Gehrig, C. A.; Hruby, V. J. *J Am Chem Soc* 1993, 115, 3399.
  35. (a) von Freyberg, B.; Schaumann, T.; Braun, W. *FANTOM User's Manual and Instructions: ETH Zürich: Zürich*, 1993; (b) von Freyberg, B.; Braun, W. *J Comput Chem* 1993, 14, 510.
  36. Meirovitch, H.; Lim, H. A. *Phys Rev A* 1989, 15, 4186.
  37. Chang, I. S.; Meirovitch, H.; Shapir, Y. *Phys Rev A* 1990, 15, 1808.
  38. Zhou, Y.; Hall, C. K.; Karplus, M. *Phys Rev Lett* 1996, 77, 2822.
  39. Kemp, J. P.; Chen, Z. Y. *Phys Rev Lett* 1998, 81, 3880.
  40. Baysal, C.; Meirovitch, H. *Biopolymers* 1999, 50, 329, and references given therein.
  41. Freyberg, B. V.; Braun, W. *J Comput Chem* 1991, 12, 1065.
  42. Meirovitch, H. *J Chem Phys* 1988, 89, 2514.